EVALUATION OF PROCESS PARAMETERS ON CUTTING FORCES AND HEAT GENERATION IN HIGH-SPEED END MILLING OF Al-Si-Mg-Fe ALLOY

[1]S. Madhava Reddy and [2]A. Chennakesava Reddy*

[1]Associate Prof., Department of Mechanical Engineering
Mahatma Gandhi Institute of Technology, Hyderabad

[2]Prof. Mechanical Engineering
JNTU College of Engineering, Hyderabad
dr_acreddy@yahoo.com

Abstract: In this paper, high-speed end milling of Al-Si-Mg-Fe alloy has been carried out. Straight flute end milling cutters (PCD) and high-pressure coolant were used for high-speed end milling of the Al-Si-Mg-Fe alloy materials. The cutting force depends upon the cutting speeds, depth of cuts and feed rates. The cutting temperature (heat generation in the Al-Si-Mg-Fe alloy) increases with an increase in the depth of cut and feed rate and decreases with an increase in the cutting speed. This behavior can be attributed to the precipitation hardening and thermal stability in the alloy. The distortion of the workpiece is not affected by the high-speed machining. The Al-Si-Mg-Fe alloy gives curled or easily broken chips.

1. INTRODUCTION

High-speed machining is a relative term from a materials perspective, since different materials are machined with different cutting speeds to insure adequate tool life. The cutting speed determines whether a material would form continuous or segmented chips. The high-speed machining is defined quantitatively in terms of cutting speed ranges [1]:

- High-speed machining (600 to 1800 m/min)
- Very high-speed machining (1800 to 18000 m/min)
- Ultra high-speed machining (18000 m/min) and above.

Salomon conducted a series of experiments in the late 1920's on nonferrous metals such as aluminum, copper and bronze at speeds up to 16,500 m/min [2]. He claimed that the cutting temperature reached a peak at a given cutting speed and as the cutting speed was further increased the temperature decreased. He also stated that the better cutting conditions could be achievable at high speeds. It was not until the late 1950's that research in high-speed machining was reborn and doubts arose about Salomon's theory [3]. From that time to the mid-1980's, the interest in high-speed machining was driven by the assumption that very high speeds could lead to local melting in the chip and subsequently reduced forces, stresses and wear on the tool. Further research showed that most metals including soft aluminum alloys turn out segmented chips at high cutting speeds [4]. The segmented chips results in a harmful fluctuating fatigue loading on the cutting edge leading to tool damage.

In recent years, the changes in the global economy and competition impose the need for cost reduction and increase in productivity throughout the machining industry. The development of new tool materials and high-speed machining spindles switches to the interest in high-speed machining. As a result, the focus has been given to:

- Increasing the cutting speed
- Controlling chip segmentation
- Reducing product distortion due to stress and heat generation during machining.

The high-speed machining is used in the defense, aerospace and automobile industries. Most aerospace manufacturers have implemented high-speed machining in end milling using small-size cutters. The most common work material was aluminum; there was no tool wear limitation, particularly when carbide cutters were used [5]. Also, in the aerospace industry, the major application of high-speed machining has been in thin walled structures. It is more economically beneficial to fabricate thin walled components by removing large amounts of material from bulk aluminum with high-speed machining instead of by casting, forming, and assembly.

In high-speed machining, all the energy associated with the cutting process is on account of either plastic deformation in the shear zone, friction along the tool rake face or the change in momentum of the chip. Generally, the shear energy and the frictional energy end up as a thermal energy. In machining, the following parameters can change the amount of thermal energy produced during the cutting process:

1. An increase in the cutting speed and the feed rate causes an increase in the temperature of chips and tool [6, 7].
2. The temperature in the primary shear zone and tool/work interface would decrease with an increase in the tool rake angle [8].
3. An increase in the undeformed chip thickness causes an increase in the thermal energy [9].

In the present work, the influence of high-speed end milling on the cutting forces and heat generation in Al-Si-Mg-Fe alloy workpieces, which were cast by the die casting method, was investigated. The end mills have cutting teeth on the end as well as on the periphery of the cutter. In the present investigation, the straight flute end-milling cutter was used for machining of Al-Si-Mg-Fe alloy workpieces.

2. DESIGN OF EXPERIMENTS

The Al-Si-Mg-Fe alloy was prepared and chemical analysis of their ingredients was done. The chemical composition of alloy is given in Table 1. The sand mould, investment shell, and cast iron mould were employed to prepare the samples for high-speed end milling.

Table-1: Chemical composition of alloys

Alloy	Composition determined spectrographically, %						
Element	Al	Si	Mg	Fe	Cu	Mn	Cr
%	85.22	9.0	2.0	3.5	0.01	0.25	0.02

2.1 Selection of the Quality Characteristics

The selection of quality characteristics to measure as experimental outputs greatly influences the number of tests that will have to be done statistically meaningful. The quality characteristics, which were selected to influence the high-speed end milling of Al-Si-Mg-Fe alloy, are the cutting forces and heat generation.

2.2 Selection of Machining Parameters

This is the most important phase of investigation. If important parameters are unknowingly left out of the experiment, then the information gained from the experiment will not be in a positive sense. The parameters, which influence the performance of the high-speed end milling, are:

- Microstructure of Al-Si-Mg-Fe alloy
- Cutting speed
- Feed rate
- Depth of cut
- Coolant

Since the high-speed milling involves high cost of machining, the process parameters were optimized using Taguchi's method [10]. Taguchi techniques offer potential savings in test time and money by more efficient testing strategies. Not only are savings in test time and cost available but also a more fully developed product or process will emerge with the use of better experimental strategies.

Table-2 Control parameters and levels

Parameter	Symbol	Level – 1	Level – 2	Level-3
Coolant pressure, bar	c	0	100	200
Cutting speed, m/min	n	300	500	700
Feed rate, mm/min	f	1000	3000	5000
Depth of cut, mm	d	0.2	0.4	0.6

2.3 Selection of Levels for Control Parameters

Control parameters are those parameters that a manufacturer can control the design of high-speed end milling. The levels chosen for the control parameters were in the operational range of the high-speed end milling. Trial runs were conducted by choosing one of the machining parameters and keeping the rest of them at constant values. The selected levels for the chosen control parameters are summarized in Table – 2. Each of the four control parameters was studied at three levels.

2.4 Assignment of Control Parameters

The orthogonal array, L_9 was selected for the high-speed end milling. The parameters were assigned to the various columns of orthogonal array (OA). The assignment of parameters along with the OA matrix is given in Table–3.

Table-3 Orthogonal Array (L_9) and control parameters

Treat No.	n	f	d	c
1	1	1	1	1
2	1	2	2	2
3	1	3	3	3
4	2	1	2	3
5	2	2	3	1
6	2	3	1	2
7	3	1	3	2
8	3	2	1	3
9	3	3	2	1

2.5 Preparation of Al-Si-Mg-Fe Alloy Melts

An Al-Si alloy was melted in an oil-fired furnace. During melting pure aluminum, pure magnesium in the solid form and pure iron in the liquid form were added to the liquid melt according to the charge calculation. The melting losses of aluminum and magnesium were taken into account while preparing the charge. During melting the charge was fluxed with coveral-11 (a Foseco company product) to prevent dressing. The molten metal was then degasified by tetrachlorethane (in solid form) using a plunger ending in a small inverted crucible. The melt was also modified with sodium in the crucible before pouring. The crucibles were made of graphite [11-14]. The dross removed melt was finally gravity poured into the preheated sand, investment and die (iron) cast moulds. The solidified cast samples were solution treated under the T6 conditions.

2.6 High-speed End Milling and Evaluation of Cutting Forces and Heat Generation

The machine used in the study is a vertical type-machining center (figure 1). High-pressure coolant was used in the high-speed milling. Straight flute end milling cutters (PCD) were used for high-speed end milling of the Al-Si-Mg-Fe alloy materials. In order to measure cutting forces, the displacement sensors were installed on the spindle unit of a high precision machining center. The spindle has

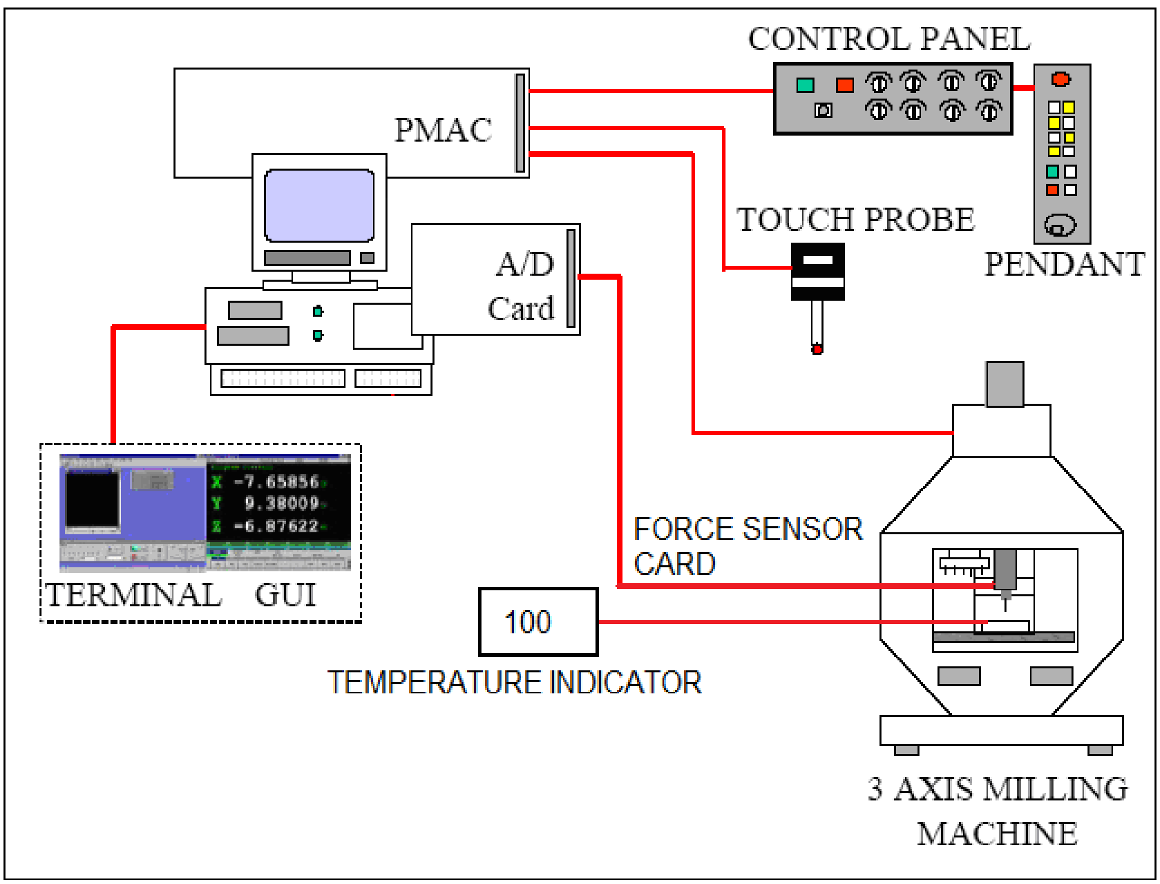

Fig.1 High-Speed Milling Center

constant position preloaded bearings with oil-air lubrication, and the maximum rotational speed is 20,000 rpm. Four eddy-current displacement sensors are installed on the housing in front of the bearings to detect the radial motion of the spindle (figure 2). The specifications of the sensor are as follows: the diameter is 5.4mm and the length is 18mm; measurement range is 1mm; nominal sensitivity is 0.2mm/V; dynamic range is 1.3kHz; linear sensitivity is ±1 % of the full scale. Figure 2 shows the sensor locations. The two sensors s1 and S3 are aligned opposite in the x-direction, and the other two S2 and S4 are aligned in the Y-direction. The resultant cutting forces were determined from the measured forces. The temperature of the workpiece material was measured using a thermocouple. The heat generated in the workpiece material was then calculated from the measured temperatures.

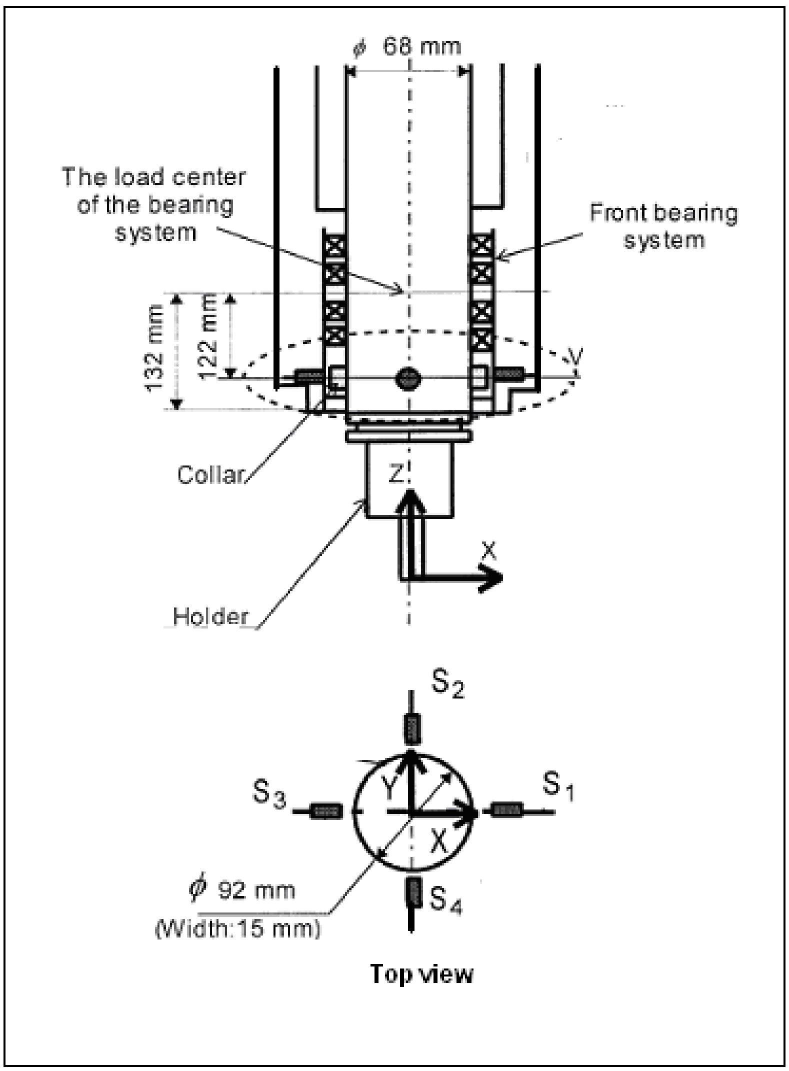

Fig.2 Arrangement of Sensors on the Spindle

2.7 Optical microscopy and transmission electron microscopy (TEM)
The optical microscopy was used to determine the grain size and shape and distribution of various phases and inclusions, which could affect the mechanical properties of the castings. The specimens to be observed under an optical microscope were prepared using standard procedures. The chips produced by the high-speed machining of Al-Si-Mg-Fe alloy were observed in a JEOL 2000 FX transmission electron microscope operated at 200kV.

2.8 Techniques to analysis results
After all tests were conducted, the decisions were made with the assistance of the following analytical techniques:

- ***Analysis of variance***: ANOVA is a statistically based, objective decision-making tool for detecting any differences in average performance of groups of items tested. The decision takes variation into account. The parameter which has Fisher's ratio (F-ratio) larger than the criterion (F- ratio from the tables) are believed to influence the average value for the population, and parameters which has an F- ratio less than the criterion are believed to have no effect on the average. Percent contribution indicates the relative power of a parameter to reduce variation.

- ***Plotting method***: To plot the effect of influential factors, the average result for each level must be calculated first. The sum of the data associated with each level in the OA column divided by the number of tests for that level would provide the appropriate averages. Plots may be made with equal increments between levels on the horizontal axes of the graphs to show the relative strengths of the factors. The strength of a factor is directly proportional to the slope of the graph.

- ***xConfirmation tests***: The key task was the determination of the preferred combination of the levels of the parameters indicated to be significant by the analytical methods. The insignificant parameters may be set at any desirable levels. The purpose of the confirmation test was to validate the conclusions drawn during the analysis phase.

3. RESULTS

The experiments were conducted randomly and repeated twice.

3.1 Effect of Process Parameters on the Cutting Forces

The cutting forces under various combinations of machining parameters are given in Table 5. The summary of ANOVA (analysis of variance) for cutting force is shown in Table 5.2. According to the analysis of variance, there are three strong parameters, which influence the cutting force. Looking at the ANOVA table, parameter d (depth of cut) has the largest effect (43.72%), parameter f (feed rate) the second largest effect (31.34%), parameter n (cutting speed) the third largest effect (24.73%), and parameter c (type of casting) has no effect.

Table 4: Experimental Results of Cutting Forces

Treat No.	Cutting Force, N	
	Trial-1	Trial-2
1	407	401
2	570	576
3	900	930
4	353	346
5	652	641
6	515	524
7	475	460
8	320	325
9	483	488

Table-5: ANOVA Summary of the Cutting Forces

Column No	Source	Sum 1	Sum 2	Sum 3	SS	v	V	F	P
1	n	3784	3031	2551	128761	2	64380.50	773.5975	24.73
2	f	2442	3084	3840	163228	2	81614.00	980.6756	31.34
3	d	2492	2816	4058	227772	2	113886.00	1368.457	43.72
4	c	3072	3120	3174	868	2	434.00	5.214953	0.20
5	e	----	----	---	749	9	83.22	-------	-------
6	T	---	----	---	521378	17	-------	-------	-------

The effect of cutting speed on the resultant cutting force is shown in figure 3. It is observed that the cutting force decreases with increase in cutting speed. This may be owing to low friction coefficient

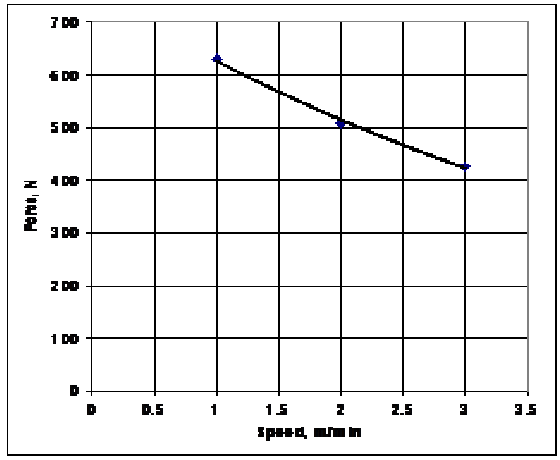

Fig 3. Variation of Cutting Force with Speed

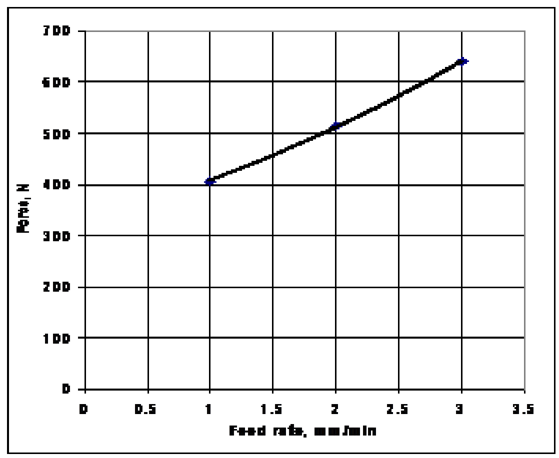

Fig 4. Variation of Cutting Force with Feed Rate

at high cutting speeds. The direction of the friction force is closely related to the direction of the chip flow angle. The cutting force increases with increase in feed rate and depth of cut (figures 4 and 5). The amount of material to be removed from the workpiece increases with increase in depth of cut and feed rate. The thickness and width of chip depend upon the amount of depth of cut and feed rate. Hence, higher depth of cuts and feed rates result in greater cutting forces. This behavior is analogous to the cutting force with increasing feed rate in oblique cutting operations previously reported by Ezugwu [15].

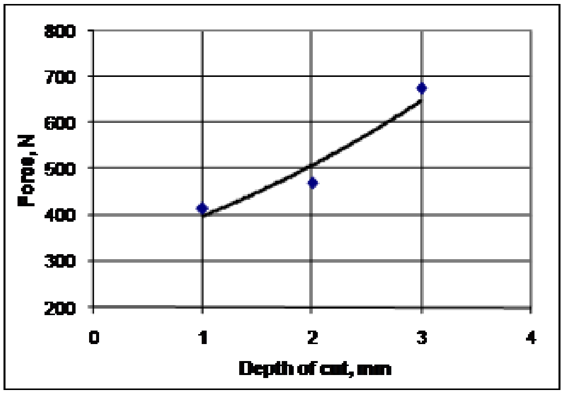

Fig 5. Variation of Cutting Force with Depth of Cut

3.2 Effect of Process Parameters on the Heat Generation

Heat generation has been estimated using measured temperatures in the workpiece. The heat generation values under various combinations of machining parameters are given in Table 4. The summary of ANOVA (analysis of variance) for heat generation is shown in Table 6. According to the analysis of variance, it can be observed that parameter d (depth of cut) has the maximum influence (55.81%) on heat generation followed by parameter f (feed rate) and parameter n (cutting speed). The cutting speed has the least effect on the heat generation in the workpiece.

Because of the very large amount of plastic strain involved in the metal cutting, it is unlikely that more than 1% of the work done is stored as elastic energy (which can be neglected), the remaining 99% would go into the chip, the tool and the work [6]. The source of major heat in the metal cutting being located at the tool tip, the temperature there would be the highest. The temperature then would conduct through the tool, work and chip. The tool is the one, which accumulates most of heat, while chip and work surfaces in contact with the tool are continuously changing. The effect of cutting speed on the heat generation is shown in figure 6. It is observed that the heat generation in the work piece decreases with increase in cutting speed. This means that the rest of the heat carried by the chip and the tool increases with increase in the cutting speed. It is reported that the temperatures in the cutting tool increases with increase in cutting speed [18]. As the heat generated in the workpiece decreases with increase in the cutting speed, the distortion in the workpiece also decreases with increase in the cutting speed. This is the great advantage of high-speed machining applied to the thin walled work materials.

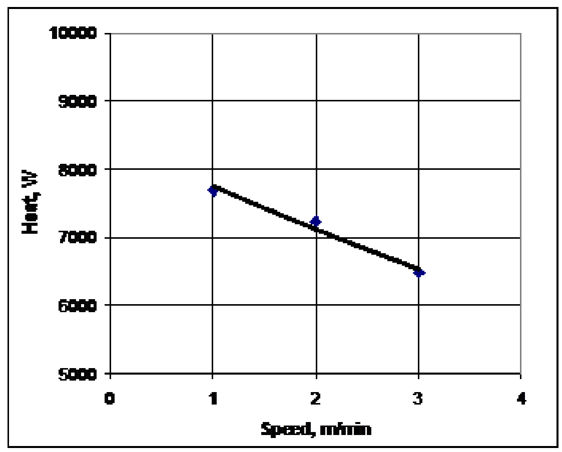

Fig 6. Variation of Heat Generation with Cutting Speed

Table 6: ANOVA Summary of Heat Generation

Column No	Source	Sum 1	Sum 2	Sum 3	SS	v	V	F	P
1	n	46119	43409	38884	4453608	2	2226804	16998.51	6.45
2	f	34180	42627	51605	25310384	2	12655192	96604.52	36.62
3	d	34295	39222	54895	38571014	2	19285507	147217.6	55.81
4	c	41454	42504	44454	772500	2	386250	2948.473	1.12
5	e	----	----	---	1179	9	131	-------	-------
6	T	----	----	----	69108686	17	--------	----=--	------

Figure 7 represents the influence of feed rate on the heat generation. The heat generation in the workpiece increases with increase in amount of feed rate. This behavior is believed to be caused by the built-up-edge (BUE) formation and the frictional forces. The variation of heat generation with depth of cut is represented in figure 8. The heat generation increases with increase in depth of cut.

3.4 Effect of Process Parameters on the Characteristics of Chips

The chip formation involves the elastic-plastic deformation, work hardening of material ahead of the cutting edge due to the plastic deformation followed by the fracture/shearing of material along the shear plane. Since the ductile materials are known to produce longer chips than the hard materials, average chip length can be used as an indirect measure of ductile/brittle fracture while machining. The size and shape of chips are given Table-7. Depth of cut and feed rate influence the characteristics of chips to the great extent. Segmented and saw-tooth chips are resulted on account of deep depth of cuts, and large feed rates. Thin and long chips are formed with the combination of fine depth of cuts and feed rates. The effect of casting condition is negligible on the characteristics of chips.

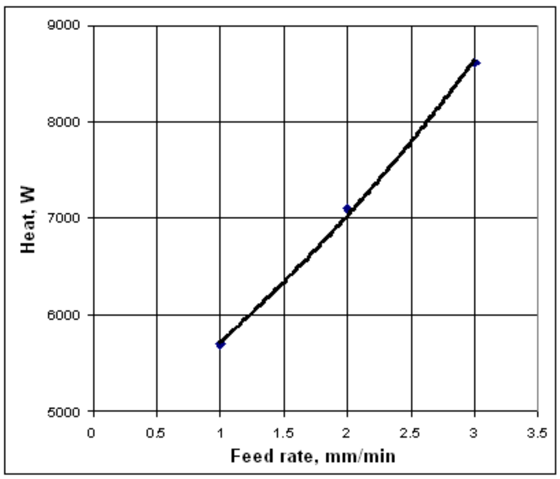

Fig 7. Variation of Heat Generation with Feed Rate

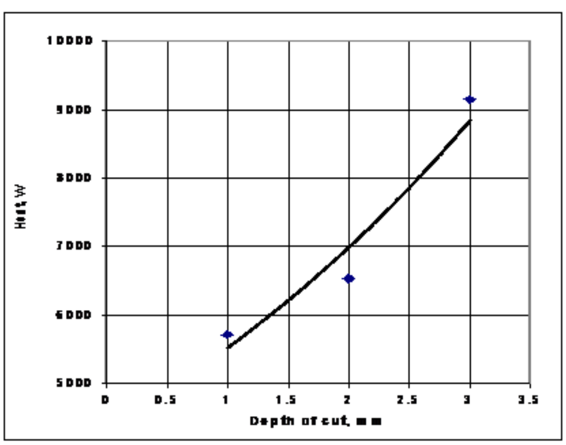

Fig 8. ariation of Heat Generation with Depth of Cut

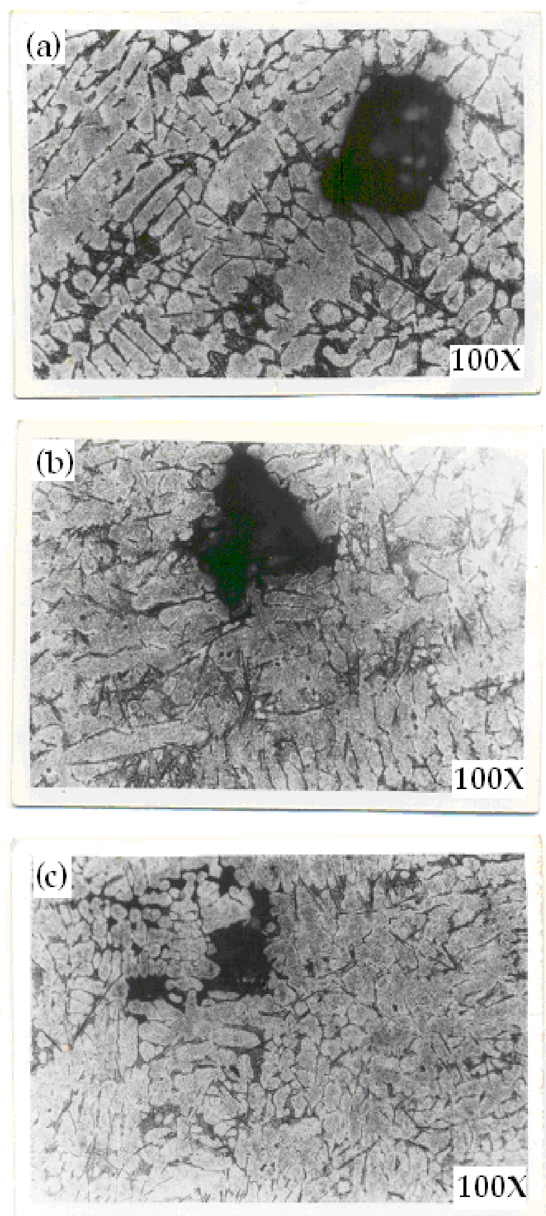

Fig 9. Microstructures of Al-Si-Mg-Fe Alloys produced by (a) Sand Cast (b) Investment Cast, and (c) Die Cast Processes.

4. DISCUSSION

The cutting force depends upon the depth of cuts and feed rates (figures 4 and 5). Also, the cutting temperature (heat generation in the workpiece) increases with an increase in the depth of cut and feed rate (figures 7 and 8). This behavior can be attributed to the precipitation hardening in the alloy owing to the formation of intermetallic compounds in Al-Si-Mg-Fe alloy (figure 9). The presence of precipitate phases is expected to impart thermal

Table 7: Size and Shape of Chips

Treat No.	Size and shape of chips	Remarks
1		Speed =300 m/min, feed rate = 1000 mm/min, depth of cut = 0.2 mm and sand cast
2, 5, 6 and 9	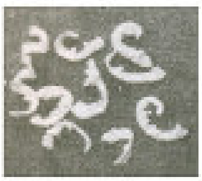	Treat-2: Speed =300 m/min, feed rate = 3000 mm/min , depth of cut = 0.4 mm and investment cast Treat-5: Speed =500 m/min, feed rate = 3000 mm/min , depth of cut = 0.6 mm and sand cast Treat-6: Speed =500 m/min, feed rate = 5000 mm/min , depth of cut = 0.2 mm and
3		Speed =300 m/min, feed rate = 5000 mm/min, depth of cut = 0.6 mm and die cast
4	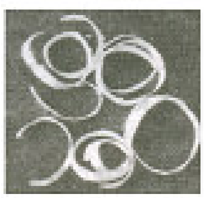	Speed =500 m/min, feed rate = 1000 mm/min, depth of cut = 0.4 mm and die cast
7	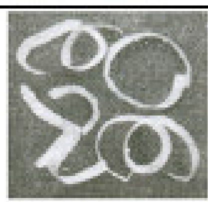	Speed =700 m/min, feed rate = 1000 mm/min, depth of cut = 0.6 mm and investment cast
8	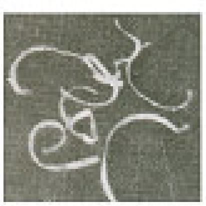	Speed =700 m/min, feed rate = 3000 mm/min, depth of cut = 0.2 mm and die cast

stability to the metallic matrix in addition to enhancing strength. The reaction products during the solidification of Al-Si-Mg-Fe alloy may be as follows:

$$\text{Liquid Melt} \quad L \rightarrow Al + Si + Mg_2Si + Al_{15}Mn_3Si_2 + Al_6FeSi + Al_5Mg_8Cu_2Si_6$$

The TEM micrographs of the chips are shown in figure 10. The formation of progressively refined, highly misoriented subgrains is observed in the deformation zone closer to the workpiece (figure 10a). The continued refinement of the microstructure is revealed in the deformation zone closer to the tool (figure 10b) and the final microstructure of the chip is shown in figure 10c. The TEM study of the microstructure of chips indicates a progressive grain refinement across the deformation zone.

The Al-Si-Mg-Fe alloy gives curled or easily broken chips (Table 7) at high cutting speeds. As the chips tended to curl considerably, the Al-Si-Mg-Fe alloy experiences the plane strain machining conditions in the high-speed milling operation.

5. CONCLUSIONS

The cutting force depends upon the cutting speeds, depth of cuts and feed rates. The cutting temperature (heat generation in the Al-Si-Mg-Fe alloy) increases with an increase in the depth of cut and feed rate and decreases with an increase in the cutting speed. This behavior can be attributed to the precipitation hardening and thermal stability in the alloy. The distortion of the workpiece is not affected by the high-speed machining. The Al-Si-Mg-Fe alloy gives curled or easily broken chips.

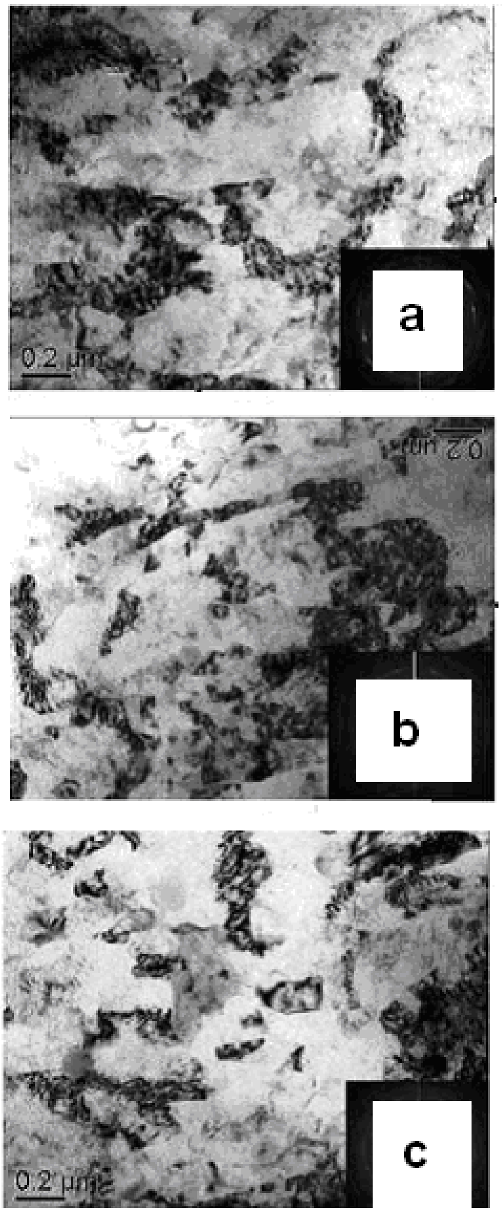

Fig 10. TEM micrographs of Partially Detached Chip Showing Progressive Grain Refinement Across the Deformation Zone

REFERENCES

1. B.F.V.Turkovich, Influence of very high cutting speed on chip formation mechanics, Proceedings of NAMRC-VII, pp.241-247, 1979.

2. C. J. Salomon, Process for the machining of metals of similarly acting materials when being worked by cutting tools, German Patent No. 523594, 1931.

3. A. O. Schimdt. Ultrahigh-speed machining. The Tool Engineer, Vol.41, pp.105-109, 1958.

4. E. M. Trent and P. K. Wright, Metal Cutting. Butterworth Heinemann, Boston, fourth edition, 2000.

5. J.R.Davis, High-speed machining, Metals Handbook. ASM, Vol.16, pp.597-606, ninth edition, 1989.

6. G. Boothroyd and W. A. Knight, Fundamentals of Machining and Machine Tools. Marcel Dekker, Inc., New York, second edition, 1989.

7. T. J. Drozda and C. Wick, editors. Machining. SME, Vol.1, 1983.

8. P. K. Wright, S. P. McCormick and T. R. Miller. Effect of rake face design on cutting tool temperature distributions, Journal of Engineering for Industry, Transactions ASME, Vol.102, pp.123-128, 1980.

9. M. C. Shaw, Metal Cutting Principles, Oxford University Press, Inc., New York, second edition, 2005.

10. A. Chennakesava Reddy, and V.M. Shamraj, Reduction of cracks in the cylinder liners choosing right process parameters by Taguchi method, Foundry, Vol.10, No.4, pp.47-50, 1998.

11. A. Iyer and P.N. Sadhu, Metal treatment practices in aluminium diecasting industry, Indian Foundry journal, Vo.45, No.8, pp.17-25, 1999.

12. K. N. Prabhu, K. Shivaprasada, and K. R. Udupa, Assessment of degree of modification in Al-Si eutectic alloy (LM6) by NDT techniques, Indian Foundry Journal, Vol.45, No.9, pp.177-183, 1999.

13. S.A. Kori, B.S. Murty, and M. Chakraborty, Grain refinement of Al-Si alloys, Indian Foundry Journal, Vol.45, No.1, pp.7-19, 1999.

14. R.H. James, Casting aluminium alloy casting process, Modern Castings, pp.9-16, July 1965.

15. E. O. Ezugwu, High speed machining of aero-engine alloys, Journal of the Brazilian Society of Mechanical Sciences & Engineering, Vol.26, No.1, pp.1-11, 2004.

16. K. M. V. Pena, J. J. Mason and M. Li, High speed temperature measurements in orthogonal cutting of aluminum, Experimental Mechanics, Vol.42, pp.221-229, 2003.